



Technical Note: Influence of building representation in flood hydrodynamic modelling: the case of the 2021 Ahr valley flood

Shahin Khosh Bin Ghomash¹, Nithila Devi Nallasamy¹, and Heiko Apel¹

¹Section Hydrology, GFZ German Research Centre for Geosciences, Potsdam (Germany)

Correspondence: Shahin Khosh Bin Ghomash (shahin@gfz-potsdam.de)

Abstract. The increasing flood risk in urban areas, driven by rising urbanization and climate change, underscores the need for accurate representation of buildings and urban features in flood hydrodynamic models. This study investigates the impact of different building representation techniques on flood hydrodynamic and impact modeling, using the 2021 flood event in the Ahr Valley, Germany. Three methods—Building Block (BB), Building Hole (BH), and Building Resistance (BR)—are applied across varying model resolutions to assess their influence on flood extent, water depths, and flow velocities.

Our findings reveal that building representation can affect both flood extent and flow dynamics. The Building Block and Building Hole approaches generally lead to larger flooded areas with deeper water and higher velocities, while increased resistance or omitting buildings results in smaller flood extents, shallower water, and slower flow. Additionally, we show a strong link between building representation and model resolution. At coarser resolutions, the Building Hole method produces the most accurate flood extents, while the increased resistance method performs better at finer scales. Our findings show that at coarser resolutions, the choice of building representation is more critical, with larger differences in flood extent across setups. We show that while all methods produce acceptable flood extents, variations in water depths and velocities highlight the importance of choosing the right building representation for accurate flood impact calculations. These variations are vital for flood impact assessments, especially in dense urban areas. Our results emphasize the importance of selecting appropriate building representation methods based on model resolution to enhance urban flood modeling and impact assessment accuracy.

1 Introduction

The changing climate is causing an increase in both the frequency and intensity of extreme weather events, resulting in more frequent and severe floods (Skougaard Kaspersen et al., 2017). Hydrodynamic models are becoming increasingly important for assessing the impact of floods and are widely used in flood management planning and risk assessments (Merz et al., 2020). However, due to the limited availability of high-resolution data and the complexity of urban landscapes, accurately modeling and forecasting urban floods remains a significant challenge for researchers and policymakers.

Uncertainties in hydrodynamic modeling can stem from various sources, such as the model structure, parameters, and boundary conditions. These factors can significantly influence the reliability and accuracy of the model's performance (Caviedes-Voullième et al., 2020; Alipour et al., 2022). Among the various sources of uncertainty related to model structure and parameters, topographic data have been recognized as one of the key factors influencing the accuracy of flood simulations (Sharma and



Regonda, 2021; Jiang et al., 2022). Catchment topographic features are known to play a significant role in controlling the spatial distribution of runoff dynamics and influencing surface runoff connectivity (Khosh Bin Ghomash et al., 2019; Nithila Devi and Kuiry, 2024). Typically in urban areas, a significant portion of the surface topography is made up of buildings. Previous research has shown that buildings can significantly impact flood volume and flow propagation through a combination of storage, obstruction, and resistance effects (Bruwier et al., 2018; Shen and Tan, 2020). Buildings walls may obstruct the flow or the flow may pass through building structures at reduced speeds if the main entrance or windows are open, or if the floodwater rises above the height of the entrance threshold. (Wang et al., 2010).

In urban flood modeling, various building treatment methods have been proposed to address these effects, including the buildings block, building resistance and building hole approaches (Schubert and Sanders, 2012; Jiang et al., 2022; Iliadis et al., 2024). In the buildings block method, the elevation of building footprints is raised to a certain height or in case of availability of detailed building data, to the rooftop level of each building. An example of this can be found at Hunter et al. (2008), where building footprints in an urban catchment area in the UK were elevated by 12 meters for larger houses and 6 meters for smaller houses. The building resistance method, as also discussed by Alcrudo (2004); Néelz and Pender (2007), increases the surface friction coefficient in areas where buildings are located. In the building hole approach, building footprints are excluded from the computational grid, functioning as reflective boundaries, which is equivalent to the building block method with infinite building heights. This method has been widely used in previous studies, e.g. Apel et al. (2022); Khosh Bin Ghomash et al. (2022, 2023, 2024b). Although various methods for representing buildings in hydrodynamic modeling are available, it is crucial for the modeler to understand which approach is most appropriate for flood simulations to ensure the highest accuracy in results.

The 2021 flooding event in the Ahr Valley, Germany, serves as a stark reminder of the devastating impact extreme weather events can have. In July 2021, the region was hit by a catastrophic flood, leading to loss of life, displacement of residents, and widespread damage to infrastructure, homes, and landscapes (Mohr et al., 2022). Of the 184 fatalities recorded in Germany, 133 occurred along the Ahr River, a tributary of the Rhine. The Ahr River basin, though relatively small (approximately 900 km²), has morphological characteristics—such as narrow streams within gorges—that limit its capacity to handle sudden surges of water. Further on the area contains the urban area of Bad Neuenahr-Ahrweiler, which is characterized by dense urban structures with a population of approximately 26,500 (Truedinger et al., 2023).

This study examines the effect of building representation on hydrodynamic modeling of this particular flood. We utilize the above mentioned three different building representation methods to evaluate their impact on predicted flood extent and flow characteristics. Firstly, the buildings block approach, where building footprints are elevated based on the height of each individual building. The height of each building was taken from the LoD1-DE dataset for Germany. The second method, the building resistance approach, where surface roughness within the building footprints is increased to varying degrees. Lastly, the building hole method, excluding building footprints from the computational grid, treating them as reflective boundaries. Moreover, as the choice of model resolution is often crucial in model setup, the representation of buildings, and is restricted by limited computational resources or the lack of high-resolution data, we investigate the interactions between these building representation methods and grid resolution by applying model resolutions ranging from $dx = 1\text{m}$ to 10m .



2 Methods

2.1 Hydrodynamic model: RIM2D

RIM2D is a two-dimensional, raster-based hydrodynamic model developed by the Section Hydrology at the German Research Centre for Geosciences (GFZ) in Potsdam, Germany. It is designed to solve the local inertia approximation of the Shallow Water equations, as outlined by Bates et al. (2010), which has proven effective for flood inundation modeling (Falter et al., 2014; Neal et al., 2011; Apel et al., 2022, 2024; Khosh Bin Ghomash et al., 2024a, b).

The local inertia formulation provides a more accurate representation of water flow dynamics compared to simpler models, such as the diffusive wave model (De Almeida and Bates, 2013; Caviedes-Voullième et al., 2020), by introducing a term that accounts for the rate of change in local fluid momentum. This term influences how momentum is transferred from one time step to the next, meaning that the flow at any given time step affects the subsequent step by requiring acceleration from its previous state. In the context of shallow water flow modeling, the local inertia approach serves as a bridge between the diffusive wave approximation and the more comprehensive full-dynamic equations.

While the original explicit numerical solution proposed by Bates et al. (2010) may become unstable under near-critical to super-critical flow conditions or with small grid cell sizes (De Almeida and Bates, 2013), RIM2D addresses these issues by incorporating the numerical diffusion method introduced by de Almeida et al. (2012).

RIM2D is written in Fortran and has been coded for massive parallelization on Graphical Processor Units (GPU) through NVIDIA CUDA Fortran libraries. The model supports computations on multiple GPUs for fast computation of high resolution or large scale models with a large number of computational raster cells.

2.2 Data and model set-up

2.2.1 Spatial data and Building representation

In this study, we utilize the DGM1 digital elevation model (DEM) provided by the German Federal Agency for Cartography and Geodesy (BKG) for model setup. This DEM, with a resolution of $dx = 1$ meter, is generated through lidar mapping of the area. To examine the interaction between building representation in the model and DEM resolution, the 1-meter DEM is also resampled by averaging into resolutions of 2, 5, and 10 meters, resulting in a total of four setups with different resolutions.

The 3D building model LoD1 Deutschland (LoD1-DE), produced by the German Federal Agency for Cartography and Geodesy (BKG), was used for buildings representation. In the LoD1 model, all buildings are represented as basic blocks, with their floor plans typically sourced from the official real estate maps. The dataset also provides the height of each individual building.

We implemented seven different building representation scenarios for this study: no building (NoB), building blocks (BB), building hole (BH), and increased building resistance by factors of 2x (BR2x), 3x (BR3x), 5x (BR5x), and 10x (BR10x). These scenarios, combined with four different resolutions, resulted in a total of 28 setups. In the NoB scenario, no buildings are included in the domain, and no modifications are made to the DEM. In the building blocks (BB) scenario, the elevation



of cells containing building footprints as in LoD1-DE is raised by the height of each building, also taken from the LoD1-DE building dataset. For buildings with missing height data, a default height of 6 meters is used. In the BH scenario, cells containing building footprints as in LoD1-DE are removed from the computational grid, functioning as closed reflective boundaries. In the increased resistance scenarios, the Manning roughness values of the cells containing building footprints are multiplied by 2, 3, 5, and 10 for the BR2x, BR3x, BR5x, and BR10x setups, respectively.

Manning roughness values for the domain were assigned according to the 2020 land cover classification of Germany, which was derived from Sentinel-2 data (Riembauer et al., 2021). Manning values of 0.055, 0.05, 0.084, 0.02, 0.035, 0.029, 0.016 [$m^{-1/3}s$] were assigned to the vegetation, water bodies, forest, built-up, bare soil, agriculture and river channel land categories respectively. These values were determined through a dedicated roughness calibration using a Monte Carlo sensitivity analysis for the 2021 flood event, which included 3000 Latin Hypercube samples (Iman and Conover, 1982) with varying roughness parameters for different land use classes. The $dx = 5m$ resolution model with buildings represented by the building hole approach was used for the calibration (Khosh Bin Ghomash et al., 2024c). The manning values that best simulated inundation extent, river water levels, and floodplain water depths were selected.

2.2.2 Flood event data for the inflow boundary

Inflow to the models is based on the reconstructed water levels (in meters above sea level) at the Altenahr gauge, provided by the flood warning center of Rhineland-Palatinate (Mohr et al., 2022). This reconstruction was necessary because the gauge was destroyed during the 2021 event. For model setup, the reconstructed water levels are applied to cells of the river cross section at the western boundary of the model domain. To account for overbank flow, additional cells adjacent to the river channel with elevations below the peak water level of the flood hydrograph were also included. Water depths are assigned to these cells only when river water levels surpass their elevations.

2.3 Performance Metrics

In order to compare the resulting simulated flood extents to the observed flood extent of the 2021 flood event, a set of metrics are employed. These metrics are computed by evaluating the maximum inundation maps of the RIM2D simulations against the observed flood extent (provided by the State Agency for the Environment (LfU – Landesamt für Umwelt) of Rhineland-Palatinate). Initially, cells are categorized based on Table 1. For this classification, RIM2D results are termed "simulated" and the 2021 observed extent "observed". A confusion map is generated from each comparison, providing the total counts for the indices presented in Table 1. These counts are then utilized to compute the domain-wide inundation metrics as illustrated in Table 2. These metrics are based on works by Wing et al. (2017) and Bernini and Franchini (2013).

3 Results and discussion

Figure 1 shows the comparison of flooded areas using the Critical Success Index (CSI), Hit Rate (HR), and Bias Percentage Indicator (BI). The indices are presented for various building scenarios: no building (NoB), buildings blocks (BB), building



		Simulated	
		Wet	Dry
Observed	Wet	True Positive (TP)	False Negative (FN)
	Dry	False Positive (FP)	True Negative (TN)

Table 1. Inundation confusion matrix. Each cell in the domain for a given simulation is compared to the corresponding cell in the observed grid and classified according to this table.

Metric	Equation	Poor	Perfect	Description
Critical Success Index	$\frac{TP}{TP + FP + FN}$	0	1	ratio of accurate wet cells to total wet cells and missed wet cells
Hit Rate	$\frac{TP}{TP + FN}$	0	1	portion of observed wet cells reproduced by the model
Bias Percentage Indicator	$100 \left(\frac{TP + FP}{TP + FN} - 1 \right)$	-100 or 100	0	relative percentage error of the final extent of the flooded area

Table 2. Flood inundation performance metrics

hole (BH), and increased building resistance by factors of 2x (BR2x), 3x (BR3x), 5x (BR5x), and 10x (BR10x), across model
 125 resolutions of $dx = 1, 2, 5,$ and 10 m. Overall, the RIM2D model demonstrates high accuracy in reproducing flood extents
 across all building scenarios, with all scenarios achieving high scores on all three indices. Even the scenario without buildings
 in the model (NoB) attains high scores (e.g., CSI scores above 0.80 in Figure 1a). Interestingly, at coarser resolutions ($dx = 5$
 and 10 m), the building hole (BH) scenario yields the highest scores across all indicators, providing the most accurate flood
 extent compared to observations, while the increased resistance scenarios show the lowest accuracy. In contrast, at higher
 130 resolutions ($dx = 1$ and 2 m), the increased resistance scenarios achieve the highest scores. These findings emphasize the strong
 correlation between building representation and model resolution. Another point to note is that the differences between the
 various building scenarios are more pronounced in the coarser setup ($dx = 10$ m) compared to the other finer resolution setups.
 This may be due to the larger cells in the coarser setup, which cause the building footprints to cover larger areas, possibly
 blocking flow paths in the urban environment. As a result, this has a greater impact on flow dynamics, compared to the finer
 135 resolution setups. This emphasizes the significance of building representation when using relatively coarser resolution models,
 which are often preferred in many instances either for their computational efficiency or due to the lack of high resolution data.

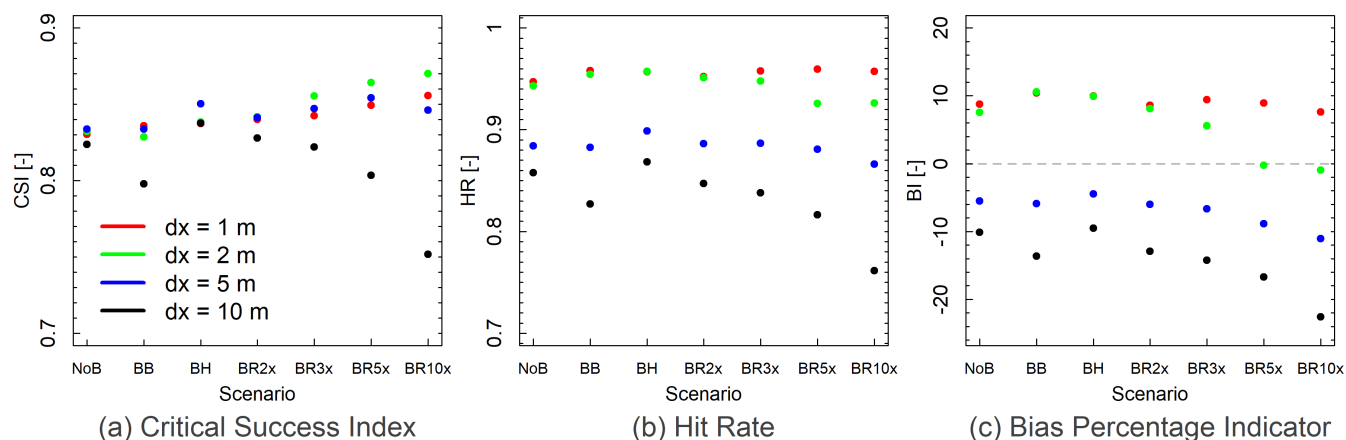


Figure 1. Comparison of flooded areas with the indices' Critical Success Index (CSI), Hit Rate (HR) and Bias Percentage Indicator (BI). The flooded areas of the building scenarios: no building (NoB), buildings blocks (BB), building hole (BH), increased building resistance of 2x (BR2x), 3x (BR3x), 5x BR(5x) and 10x (BR10x) for model resolutions $dx = 1, 2, 5$ and 10 m are presented.

Differences in flooded areas are also observed when comparing the maximum flooded areas across the various scenarios. For instance, in the $dx = 5$ m setup, areas with water depths greater than 1 cm span 11.63, 11.00, 11.11, 11.57, 11.49, 11.23, and 10.96 km^2 for the NoB, BB, BH, BR2x, BR3x, BR5x, and BR10x scenarios, respectively. These values are expected, as in scenarios like NoB and the building resistance scenarios, which did not involve processing of building cell elevations, the cells on the building footprints are also flooded which leads to a higher number of wet cells and therefore more flooded areas. To have a more robust comparison, this time we exclude the cells overlapping with building footprints. This adjustment results in flooded areas with water depths exceeding 1 cm for the NoB, BB, BH, BR2x, BR3x, BR5x, and BR10x scenarios being 10.99, 10.95, 11.11, 10.93, 10.85, 10.60, and 10.34 km^2 , respectively. In this case, it is seen that the BH scenario results in the largest flooded area. However still the differences among the different model setups are generally small in terms of simulated flood extents.

To better understand how each building representation method influences flood extent, Figure 2 displays the maximum inundated areas with water depths exceeding 1 cm and 100 cm for the following building scenarios: no building (NoB), building blocks (BB), building hole (BH), and increased building resistance by 2x (BR2x), 3x (BR3x), 5x (BR5x), and 10x (BR10x), across model resolutions of $dx = 1, 2, 5,$ and 10 m. To allow for a clearer comparison, inundated cells corresponding to building footprints are excluded. The most significant differences in flood extent among the building scenarios occur in the coarser $dx = 10$ m setup, emphasizing the critical role of building representation techniques in coarser resolution models. Additionally, the scenarios with increased surface resistance show the greatest deviation from the other setups. It is also observed that at greater water depths (Figure 2b), the slope of the lines becomes slightly steeper at coarser resolutions. This indicates that the representation of buildings causes slightly larger differences in flooded areas at higher water depths compared to lower ones.

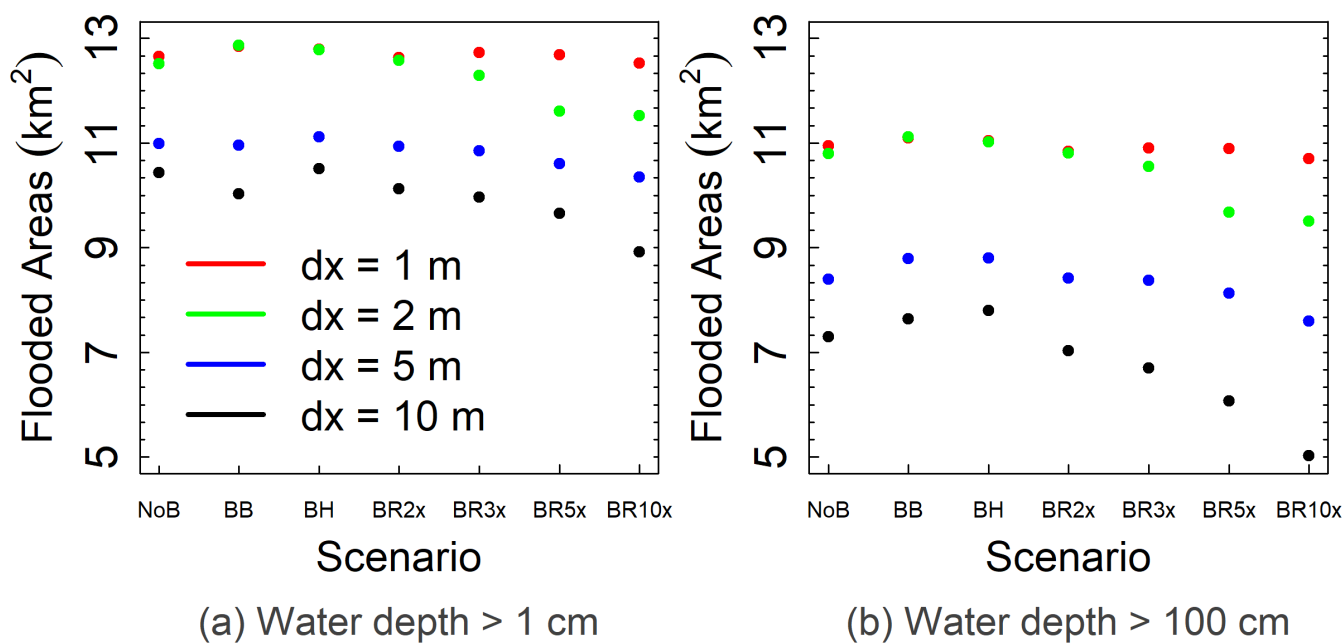


Figure 2. Maximum inundated areas with water depths above 1 and 100 cm for the building scenarios: no building (NoB), buildings blocks (BB), building hole (BH), increased building resistance of 2x (BR2x), 3x (BR3x), 5x BR(5x) and 10x (BR10x) for model resolutions $dx = 1, 2, 5$ and 10 m.

Although it is seen that the different building representations result in relatively similar flood extents, the differences become noticeable when inspecting the flood maps in detail. Figure 3 presents a close-up of the Ahrweiler region, showing the maximum water depth for various building scenarios: no building (NoB) (top left), building blocks (BB) (top right), building hole (BH) (bottom left) and increased building resistance by 10x (BR10x) (bottom right) for a model resolution of $dx = 5$ m.

160 It is seen that the NoB scenario results in a smaller flood extent compared to the other scenarios. In the BB and BH cases, the larger flooded areas may be attributed to the same volume of water spreading over a smaller space and going through narrower and more distinct flow paths (i.e. mainly streets), which is the result of the removal or elevation of building footprints. Similarly to the NoB scenario, increased roughness resistance leads to a smaller flood extent. This is due to the higher roughness of the building footprint cells, which in term can slow down the spread of the flood, causing the flow to cover a shorter distance.

165 However, based on Figure 2 the differences in flood extents are not very significant. As seen in Figure 3, there are differences in simulated water depths, with the BB and BH scenarios showing greater depths, particularly in comparison to the NoB and increased resistance configurations. This can be attributed to the reduced flow area caused by the exclusion or elevation of buildings in the BH and BB setups, which leads to the concentration of higher water levels in the remaining narrower flow paths. In the NoB and BR scenarios the water volume is also distributed over a larger area, generally leading to lower water

170 depths. Additionally, it should be noted that the flood paths in the NoB and building resistance scenarios are likely more dispersed, as these configurations allow for the redistribution of water over building footprints and involve fewer flow-blocking



situations. Since water depths and flooded areas are commonly used as input data for flood impact and risk assessments, our results demonstrate that the representation of buildings in the model can significantly influence the outcomes of these analyses.

To determine which scenarios yield the most accurate water depth estimates, we compare the observed water depths reported by residents at 65 locations (Apel et al., 2022) with the simulated water depths at those points across different scenarios for the $dx = 5$ m setup. The Bias is calculated as follows:

$$\text{Bias} = \frac{1}{n} \sum_{i=1}^n (\hat{y}_i - y_i)$$

Where:

- n is the total number of observations.
- \hat{y}_i represents the simulated values.
- y_i represents the observed values.

This yields Bias values of -0.411, 0.061, -0.039, -0.333, -0.303, -0.315, and -0.410 for the NoB, BB, BH, BR2x, BR3x, BR5x, and BR10x representation setups, respectively. These results clearly indicate that the BB and BH setups provide the most accurate water depth estimates. In contrast, the increased resistance setup with the highest roughness increase (BR10x), as well as the configuration where no building is represented (NoB), lead to the least accurate estimates.

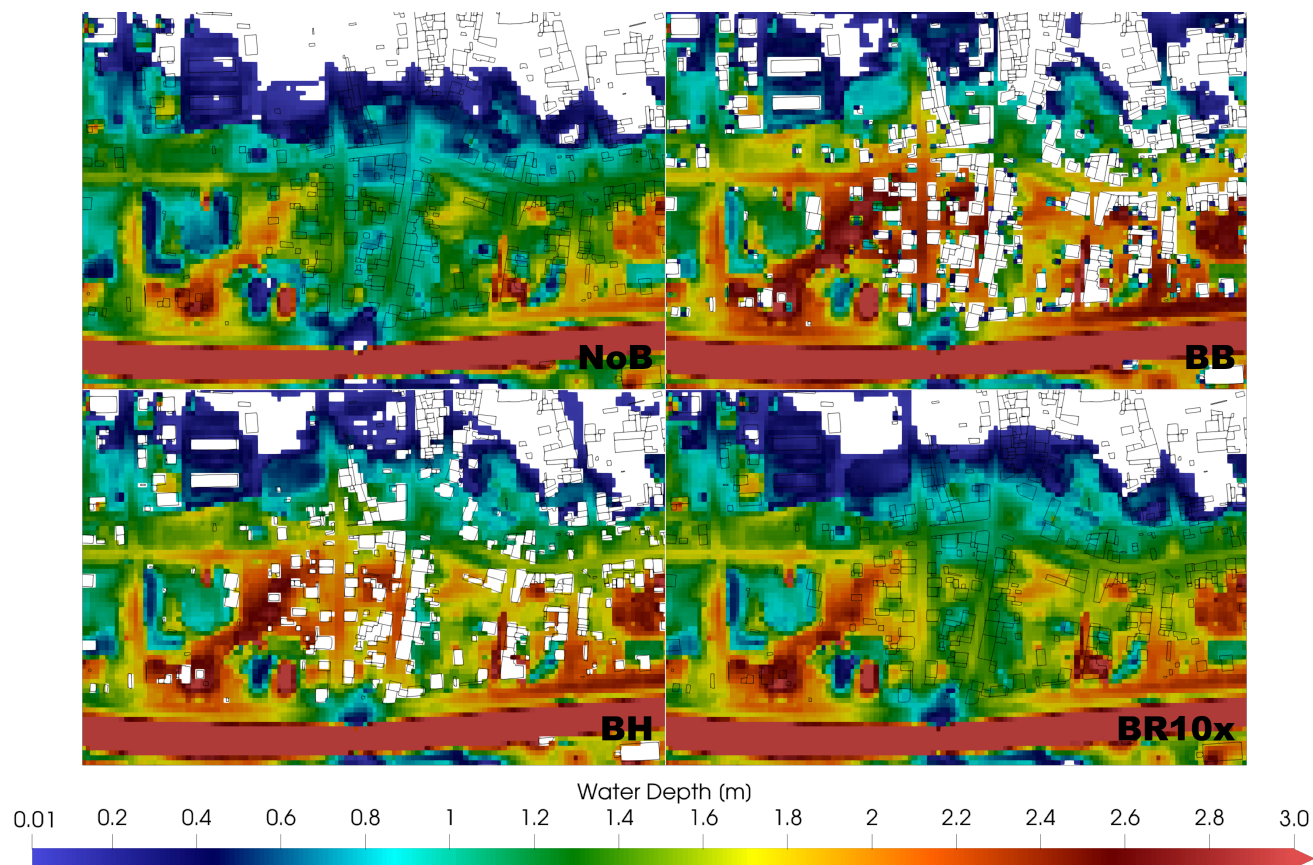


Figure 3. Detailed view at Ahrweiler of the maximum water depth of the building scenarios: no building (NoB) (top left), buildings blocks (BB) (top right), building hole (BH) (bottom left) and increased building resistance of 10x (BR10x) (bottom right) for model resolution $dx = 5$ m. Black lines represent building footprints based on the LoD1-DE dataset

And it's not just the variations in water depths across different building representations; differences in flow velocities are also observed, as expected from the model setups. Figure 4 provides a detailed view of the maximum water velocity in Ahrweiler for the building scenarios: no building (NoB) (top left), building blocks (BB) (top right), building hole (BH) (bottom left), and increased building resistance by 10x (BR10x) (bottom right), all with a model resolution of $dx = 5$ m. Significant differences in water velocities are apparent among the four setups. The NoB configuration shows evenly distributed velocities ranging from 2 to 4 m/s, while the BB and BH setups reveal more concentrated, faster flows, with velocities exceeding 4 m/s. The BR10x scenario demonstrates that increasing the roughness Manning value in the building footprint drastically reduces flow velocities, with all cells registering velocities below 2 m/s. Flow velocity is a critical factor in calculating many flood impact indicators, such as human instability or floating car maps (Apel et al., 2022). Our findings clearly indicate that the choice of building representation can substantially influence simulated urban flood water flows, ultimately affecting the outcomes of flood impact and risk assessments.



To obtain a more quantitative understanding of the differences among various building representations in terms of water depth and velocity, Figure 5 illustrates the flooded areas within the built-up regions of the area at different levels of water depth (a) and velocity (b) across multiple building scenarios: no building (NoB), building blocks (BB), building holes (BH), and increased building resistance by factors of 2x (BR2x), 3x (BR3x), 5x (BR5x), and 10x (BR10x). These values are normalized relative to the no building (NoB) scenario. The results correspond to setups with a resolution of $dx = 5$ m. Differences of up to 90 percent are observed in flooded areas with varying water depths, and up to 30 percent in areas with differing velocities. The increased resistance scenarios tend to have larger flooded areas at lower water depths, whereas the BB and BH setups result in more flooding at higher water depths. This aligns with previous figures indicating that the BB and BH setups generally result in more cells with greater water depths in the simulations. In terms of flow velocity, the increased resistance scenarios exhibit more flooded areas with flow speeds below 1 m/s, while the BB and BH setups cover more areas with flow velocities exceeding 1 m/s. Again indicating that the BB and BH setups result in faster and more realistic flow dynamics compared to the increased resistance representation approach. Overall, these findings are in line with Néelz and Pender (2007), stating that the increased resistance approach might be sufficient in simulating flood extent, but will like give grossly wrong flood dynamics in the urban environment.

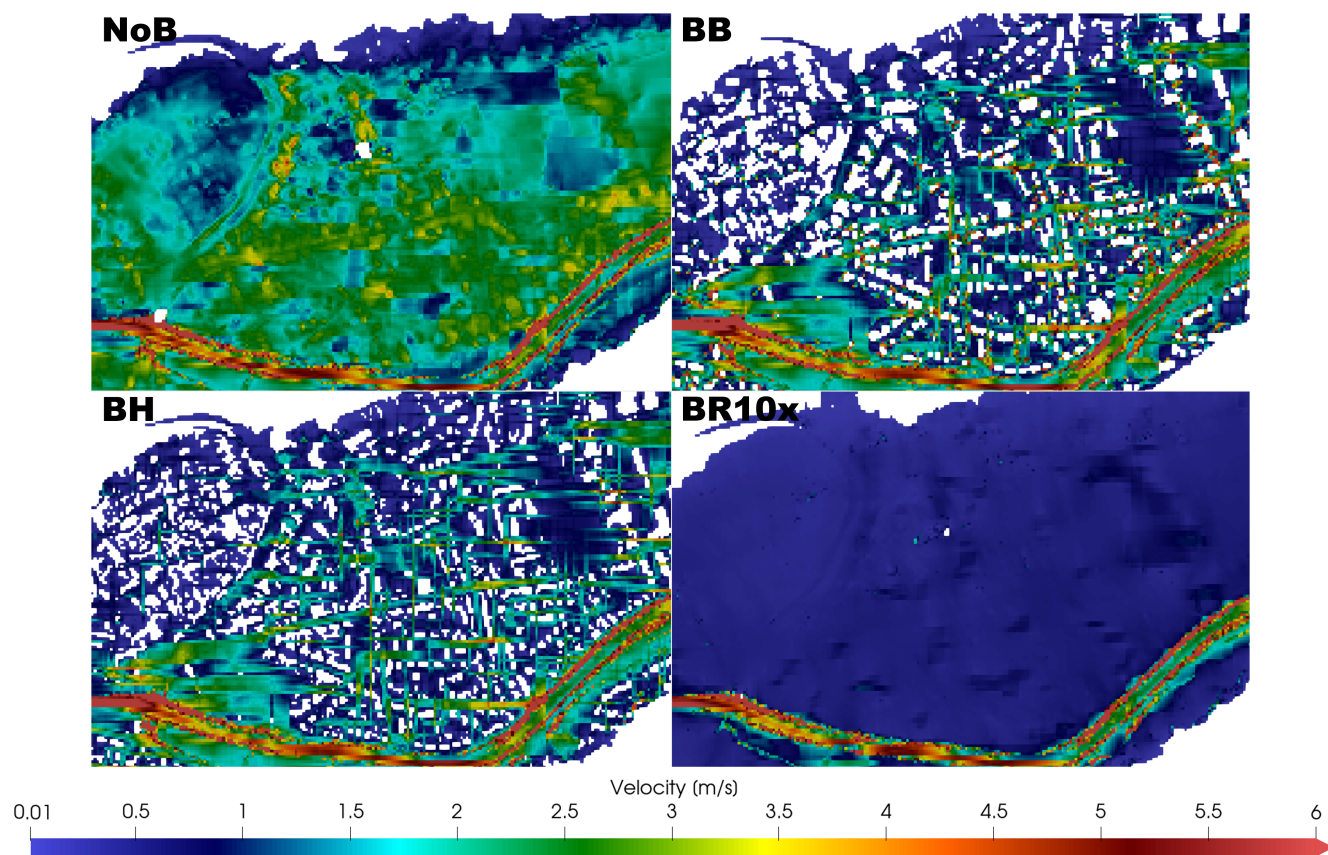


Figure 4. Detailed view at Ahrweiler of the maximum water velocity of the building scenarios: no building (NoB) (top left), buildings blocks (BB) (top right), building hole (BH) (bottom left) and increased building resistance of 10x (BR10x) (bottom right) for model resolution $dx = 5$ m.

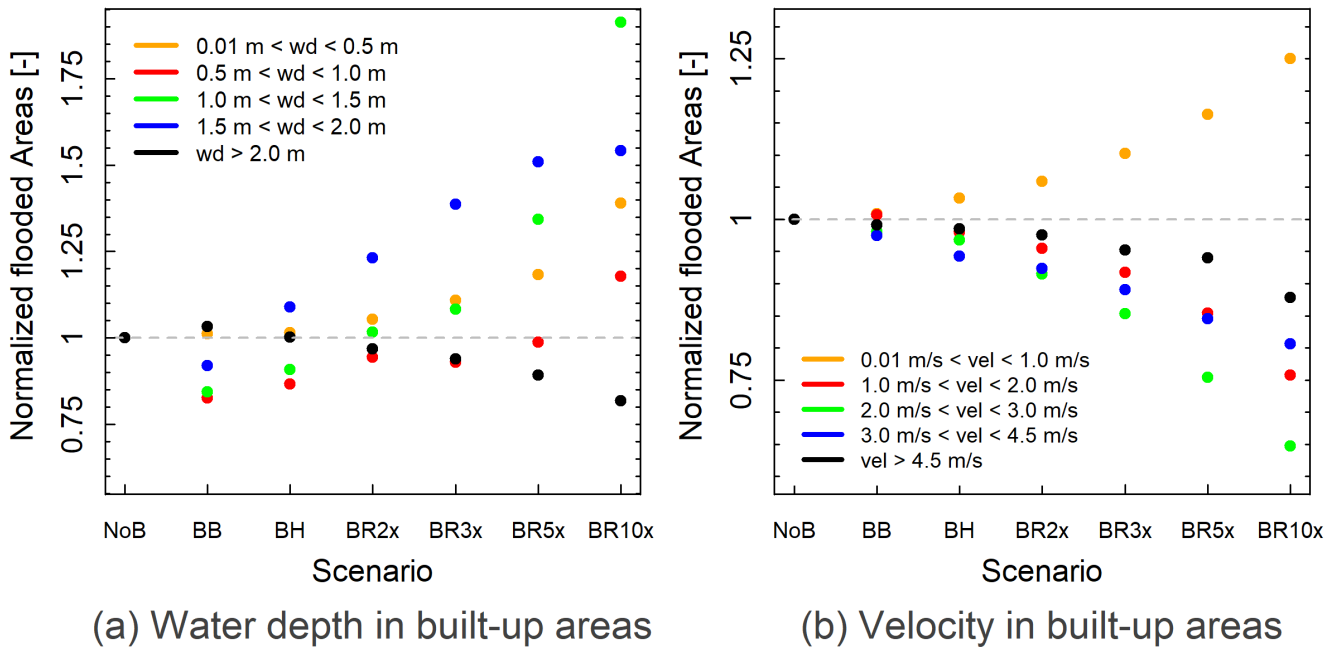


Figure 5. Flooded areas in built-up regions with different levels of maximum water depths (a) and maximum flow velocities (b) for building scenarios: no building (NoB), buildings blocks (BB), building hole (BH), increased building resistance of 2x (BR2x), 3x (BR3x), 5x BR(5x) and 10x (BR10x), normalized by the no building (NoB) scenario. The results are for the $dx = 5$ m setups.

To illustrate how different building representations can influence flood impact calculations, we generated human instability maps based on the simulated water depths and velocities in each setup, following the method outlined by Jonkman and Penning-Rowsell (2008). A conservative critical threshold of $1 \text{ m}^2 \text{ s}^{-1}$ was selected, indicating the potential instability of lightweight persons, but also to account for imperfections in the flow velocity simulations. For the NoB, BH, and BR10x setups, the areas where people may become unstable during the flood amounts to 9.81, 9.03, and 6.4 km^2 respectively. These values are calculated for the $dx = 5$ m setup. As an example, Figure 6 provides a detailed view of the human instability indicator in a segment of Ahrweiler for the building scenarios: no building (NoB) (left), building hole (BH) (center), and increased building resistance by 10x (BR10x) (right), all with a model resolution of $dx = 5$ m. Clear differences are evident among the three depicted scenarios. The BR10X representation results in significantly fewer areas of human instability compared to the BH and NoB scenarios, due to variations in the simulated water depths and velocities across these setups. Our results suggest that the choice of building representation method can greatly affect flood impact simulations and, consequently, risk assessment outcomes.

Lastly, since computational time is a key factor in selecting data for hydrodynamic models, it's important to highlight that the different building representations lead to only minor variations in computational cost. With the simulation runtimes on a single Nvidia A100 GPU being approximately in the range of 5, 28, 321, and 1554 minutes for grid resolutions of 10, 5, 2,



and 1 meter, respectively. Naturally, these times can be significantly reduced by increasing the number of GPUs used in the simulations.

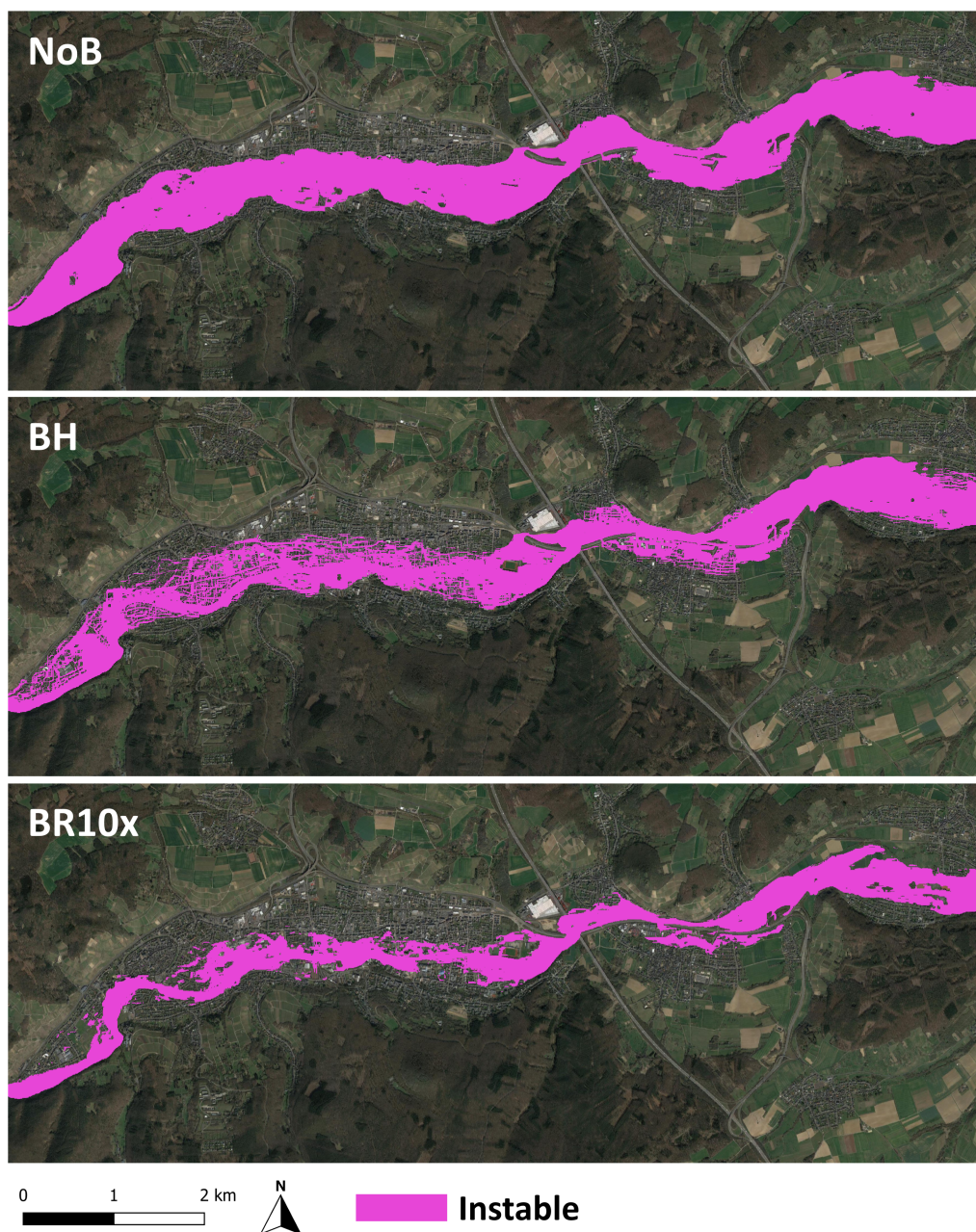


Figure 6. Detailed view at Ahrweiler of the human instability indicator for the building scenarios: no building (NoB) (left), building hole (BH) (center) and increased building resistance of 10x (BR10x) (right) for model resolution $dx = 5$ m. The critical value for human instability was set to $1 \text{ m}^2 \text{ s}^{-1}$, following Jonkman and Penning-Rowsell (2008). Satellite imagery: © Google Earth 2024.



4 Conclusions

This study assessed the influence of different building representation techniques on flood hydrodynamic modeling outcomes, using the 2021 Ahr Valley flood as a test case. By evaluating three building representation methods—Building Block (BB), Building Hole (BH), and Building Resistance (BR)—across various model resolutions, we demonstrated that the choice of building representation plays a significant role particularly for the simulation of water depths and flow velocities.

Our findings indicate that while all building representation scenarios generally produced reasonable flood extents, there were substantial variations in the finer details of water depth and velocity distributions. The BB and BH methods consistently resulted in greater water depths and higher velocities, especially in urban areas where buildings obstructed or redirected floodwaters. These variations can have profound implications for flood impact assessments, as deeper and faster-flowing water can lead to more severe flood impacts, such as heightened risks of human instability, infrastructure damage, and increased flood hazard zones.

Furthermore, the study revealed a strong interaction between model resolution and building representation accuracy. At coarser resolutions (e.g., $dx = 10$ m), the BH method emerged as the most reliable approach, producing the most accurate flood extent predictions when compared to observed flood data. This is likely due to the BH method's ability to account for the physical blocking effect of buildings, even when individual structures are less precisely defined at coarser scales. In contrast, at finer resolutions (e.g., $dx = 1-2$ m), the increased resistance method provided slightly better flood extent predictions in the presented case study. This comes, however, at the cost of large deviations of the simulated water depths compared to observed flood marks. It is reasonable to assume that this also holds true for the simulated water depths, although validation data for flow velocities are not available. But since the flow velocity is largely dominated by water surface gradients and water depths, which are validated to be better with the Bh and BB setups, it is reasonable to assume that the flow velocities simulated with the Bh and BB approaches are much closer to the actual flow dynamics of the event. This insight is critical for practitioners, as it highlights that the optimal building representation method is resolution-dependent, with implications for both data availability and computational resource management in flood modeling projects.

The study also underscores the potential risks of oversimplifying building representation in flood modeling. Simplified approaches, such as omitting buildings or using a uniform resistance factor, may lead to underestimations or overestimations of flood impacts, particularly in densely built-up areas. Given that water depths and velocities directly inform flood risk assessments and potentially also flood forecasts, such inaccuracies could lead to significant errors in evaluating potential flood damage, human safety, and emergency response planning.

In practical terms, this research provides important guidance for flood risk practitioners and modelers. If flood extent is the only concern, then a coarse resolution model with an increased resistance approach might be an appropriate choice. For all other applications, where the flood dynamics are important, the BH or BB approaches should be used. The resolution to be chosen depends on the actual problem at hand, but from the presented results, 5 m resolution might be sufficient to represent the urban flood dynamics in typical Central European settings.



In conclusion, the presented study and literature highlight the importance of the representation of buildings urban flood modeling, affecting the accuracy and reliability of flood extent and flow dynamics simulation as well as impact assessments. Although this is shown for a single case study only, the supporting literature and the underlying theoretical considerations support a generalization of this finding beyond the test study.

265 For even more realistic urban flow simulations, future studies should consider more complex building representations that account for factors such as building porosity and flow-through effects, which could further refine flood modeling accuracy in complex urban landscapes. Additionally, expanding this research to different flood events, urban configurations, and building structures will help establishing a larger empirical database for generalized guidelines for selecting appropriate building representation methods. By incorporating these considerations, hydrodynamic models can better inform flood risk manage-
270 ment, adaptation planning, and mitigation strategies, ultimately contributing to more resilient urban communities in the face of increasing flood hazards driven by climate change and urbanization.

Code availability. RIM2D is available at <https://git.gfz-potsdam.de/hydro/rfm/rim2d> (last access: 08 October 2024). RIM2D is open-source for scientific use under the EUPL1.2 license. Access is granted upon request. The simulations were performed with version 0.2.

Data availability. The land cover raster, which was used to assign roughness values to the simulation domain, is openly accessible at
275 <https://www.mundialis.de/en/germany-2020-land-cover-based-on-sentinel-2-data/> (last access: 08 October 2024).

The 1m DTM has recently been made available at <https://gdz.bkg.bund.de/index.php/default/digitale-geodaten/digitale-gelandemodelle/digitales-oberfaechenmodell-dom1.html> (last access: 08 October 2024).

Flood extent data were obtained from the UFZ data investigation portal via <https://doi.org/10.48758/ufz.14607> (Najafi et al., 2024).

The LoD1-DE building dataset can be requested and attained from the German Federal Agency for Cartography and Geodesy (BKG) via
280 <https://gdz.bkg.bund.de/index.php/default/3d-gebaudemodelle-lod1-deutschland-lod1-de.html> (last access: 08 October 2024)

Acknowledgements. This research was performed within the frame of the DIRECTED project (<https://directedproject.eu/>). Funding of the DIRECTED project within the European Union's Horizon Europe – the Framework Programme for Research and Innovation (grant agreement No. 101073978, HORIZON-CL3-2021-DRS-01) is gratefully acknowledged. This work utilized high-performance computing resources made possible by funding from the Ministry of Science, Research and Culture of the State of Brandenburg (MWFK) and are operated by the
285 IT Services and Operations unit of the Helmholtz Centre Potsdam.

Author contributions. SKBG: Conceptualization, Methodology, Investigation, Simulation, Software, Analysis, Visualization, Writing; NDN: Conceptualization, Investigation, Review; HA: RIM2D Software, Conceptualization, Review

<https://doi.org/10.5194/hess-2024-314>
Preprint. Discussion started: 4 December 2024
© Author(s) 2024. CC BY 4.0 License.



Competing interests. The authors declare no conflicts of interests.



References

- 290 Alcrudo, F.: Mathematical modelling techniques for flood propagation in urban areas, Project report: IMPACT Project, 2004.
- Alipour, A., Jafarzadegan, K., and Moradkhani, H.: Global sensitivity analysis in hydrodynamic modeling and flood inundation mapping, *Environmental Modelling & Software*, 152, 105 398, 2022.
- Apel, H., Vorogushyn, S., and Merz, B.: Brief communication: Impact forecasting could substantially improve the emergency management of deadly floods: case study July 2021 floods in Germany, *Natural Hazards and Earth System Sciences*, 22, 3005–3014, 295 <https://doi.org/10.5194/nhess-22-3005-2022>, 2022.
- Apel, H., Benisch, J., Helm, B., Vorogushyn, S., and Merz, B.: Fast urban inundation simulation with RIM2D for flood risk assessment and forecasting, *Frontiers in Water*, 6, 1310 182, 2024.
- Bates, P. D., Horritt, M. S., and Fewtrell, T. J.: A simple inertial formulation of the shallow water equations for efficient two-dimensional flood inundation modelling, *Journal of Hydrology*, 387, 33–45, <https://doi.org/10.1016/j.jhydrol.2010.03.027>, 2010.
- 300 Bernini, A. and Franchini, M.: A rapid model for delimiting flooded areas, *Water resources management*, 27, 3825–3846, 2013.
- Bruwier, M., Mustafa, A., Aliaga, D. G., Archambeau, P., Erpicum, S., Nishida, G., Zhang, X., Piroton, M., Teller, J., and Dewals, B.: Influence of urban pattern on inundation flow in floodplains of lowland rivers, *Science of the Total Environment*, 622, 446–458, 2018.
- Caviedes-Voullième, D., Fernández-Pato, J., and Hinz, C.: Performance assessment of 2D Zero-Inertia and Shallow Water models for simulating rainfall-runoff processes, *Journal of hydrology*, 584, 124 663, 2020.
- 305 De Almeida, G. A. and Bates, P.: Applicability of the local inertial approximation of the shallow water equations to flood modeling, *Water Resources Research*, 49, 4833–4844, 2013.
- de Almeida, G. A., Bates, P., Freer, J. E., and Souvignet, M.: Improving the stability of a simple formulation of the shallow water equations for 2-D flood modeling, *Water Resources Research*, 48, 2012.
- Falter, D., Dung, N., Vorogushyn, S., Schröter, K., Hundecha, Y., Kreibich, H., Apel, H., Theisselmann, F., and Merz, B.: Continuous, large-scale simulation model for flood risk assessments: proof-of-concept, *Journal of Flood Risk Management*, 9, 3–21, 310 <https://doi.org/10.1111/jfr3.12105>, 2014.
- Hunter, N. M., Bates, P., Neelz, S., Pender, G., Villanueva, I., Wright, N., Liang, D., Falconer, R. A., Lin, B., Waller, S., et al.: Benchmarking 2D hydraulic models for urban flooding, in: *Proceedings of the institution of civil engineers-water management*, vol. 161, pp. 13–30, Thomas Telford Ltd, 2008.
- 315 Iliadis, C., Glenis, V., and Kilsby, C.: Representing buildings and urban features in hydrodynamic flood models, *Journal of Flood Risk Management*, 17, e12 950, 2024.
- Iman, R. L. and Conover, W. J.: A distribution-free approach to inducing rank correlation among input variables, *Communications in Statistics - Simulation and Computation*, 11, 311–334, <https://doi.org/10.1080/03610918208812265>, 1982.
- Jiang, W., Yu, J., Wang, Q., and Yue, Q.: Understanding the effects of digital elevation model resolution and building treatment for urban 320 flood modelling, *Journal of Hydrology: Regional Studies*, 42, 101 122, 2022.
- Jonkman, S. and Penning-Rowsell, E.: Human instability in flood flows 1, *JAWRA Journal of the American Water Resources Association*, 44, 1208–1218, 2008.
- Khosh Bin Ghomash, S., Caviedes-Voullième, D., and Hinz, C.: Effects of erosion-induced changes to topography on runoff dynamics, *Journal of Hydrology*, 573, 811–828, 2019.



- 325 Khosh Bin Ghomash, S., Bachmann, D., Caviedes-Voullième, D., and Hinz, C.: Impact of rainfall movement on flash flood response: A synthetic study of a semi-arid mountainous catchment, *Water*, 14, 1844, 2022.
- Khosh Bin Ghomash, S., Bachmann, D., Caviedes-Voullième, D., and Hinz, C.: Effects of Within-Storm Variability on Allochthonous Flash Flooding: A Synthetic Study, *Water*, 15, 645, 2023.
- Khosh Bin Ghomash, S., Apel, H., and Caviedes-Voullième, D.: Are 2D shallow-water solvers fast enough for early flood warning? A comparative assessment on the 2021 Ahr valley flood event, *Natural Hazards and Earth System Sciences*, 24, 2857–2874, 2024a.
- 330 Khosh Bin Ghomash, S., Apel, H., Schröter, K., and Steinhausen, M.: Brief Communication: Rapid high-resolution flood impact-based early warning is possible with RIM2D: a showcase for the 2023 pluvial flood in Braunschweig, *Natural Hazards and Earth System Sciences Discussions*, 2024, 1–20, 2024b.
- Khosh Bin Ghomash, S., Yeste, P., Apel, H., and Nguyen, V. D.: Monte-Carlo based sensitivity analysis of the RIM2D hydrodynamic model for the 2021 flood event in Western Germany, *Natural Hazards and Earth System Sciences Discussions*, 2024, 1–25, <https://doi.org/10.5194/nhess-2024-77>, 2024c.
- 335 Merz, B., Kuhlicke, C., Kunz, M., Pittore, M., Babeyko, A., Bresch, D. N., Domeisen, D. I., Feser, F., Koszalka, I., Kreibich, H., et al.: Impact forecasting to support emergency management of natural hazards, *Reviews of Geophysics*, 58, e2020RG000 704, 2020.
- Mohr, S., Ehret, U., Kunz, M., Ludwig, P., Caldas-Alvarez, A., Daniell, J. E., Ehmele, F., Feldmann, H., Franca, M. J., Gattke, C., et al.: A multi-disciplinary analysis of the exceptional flood event of July 2021 in central Europe. Part 1: Event description and analysis, *Natural Hazards and Earth System Sciences Discussions*, 2022, 1–44, 2022.
- 340 Najafi, H., Shrestha, P., Rakovec, O., Thober, S., Kumar, R., and Samaniego-Eguiguren, L.: Data and Scripts for Advancing a High-Resolution Impact-based Early Warning System for Riverine Flooding, *Helmholtz-Centre for Environmental Research [code and data set]*, 2024.
- Neal, J., Schumann, G., Fewtrell, T., Budimir, M., Bates, P., and Mason, D.: Evaluating a new LISFLOOD-FP formulation with data from the summer 2007 floods in Tewkesbury, UK, *Journal of Flood Risk Management*, 4, 88–95, <https://doi.org/10.1111/j.1753-318x.2011.01093.x>, 2011.
- 345 Néelz, S. and Pender, G.: Sub-grid scale parameterisation of 2D hydrodynamic models of inundation in the urban area, *Acta Geophysica*, 55, 65–72, 2007.
- Nithila Devi, N. and Kuiry, S. N.: A novel local-inertial formulation representing subgrid scale topographic effects for urban flood simulation, *Water Resources Research*, 60, e2023WR035 334, 2024.
- 350 Riembaauer, G., Weinmann, A., Xu, S., Eichfuss, S., Eberz, C., and Neteler, M.: Germany-wide Sentinel-2 based land cover classification and change detection for settlement and infrastructure monitoring, in: *Proceedings of the 2021 Conference on Big Data from Space*, Virtual, pp. 18–20, 2021.
- Schubert, J. E. and Sanders, B. F.: Building treatments for urban flood inundation models and implications for predictive skill and modeling efficiency, *Advances in Water Resources*, 41, 49–64, 2012.
- 355 Sharma, V. C. and Regonda, S. K.: Two-dimensional flood inundation modeling in the Godavari River Basin, India—Insights on model output uncertainty, *Water*, 13, 191, 2021.
- Shen, J. and Tan, F.: Effects of DEM resolution and resampling technique on building treatment for urban inundation modeling: a case study for the 2016 flooding of the HUST campus in Wuhan, *Natural Hazards*, 104, 927–957, 2020.
- 360 Skougaard Kaspersen, P., Høegh Ravn, N., Arnbjerg-Nielsen, K., Madsen, H., and Drews, M.: Comparison of the impacts of urban development and climate change on exposing European cities to pluvial flooding, *Hydrology and Earth System Sciences*, 21, 4131–4147, 2017.



- Wang, X., Cao, Z., Pender, G., and Neelz, S.: Numerical modelling of flood flows over irregular topography, in: Proceedings of the Institution of Civil Engineers-Water Management, vol. 163, pp. 255–265, Thomas Telford Ltd, 2010.
- 365 Wing, O. E., Bates, P. D., Sampson, C. C., Smith, A. M., Johnson, K. A., and Erickson, T. A.: Validation of a 30 m resolution flood hazard model of the conterminous United States, *Water Resources Research*, 53, 7968–7986, 2017.